

# Supplements

Robin Ekelund<sup>1</sup> and Patrick Eriksson<sup>1</sup>

<sup>1</sup>Department of Space, Earth and Environment, Chalmers University of Technology, Gothenburg, Sweden.

November 8, 2018

## 1 2 mm data, omitted parameters

Fig. 1, 2, 3 and 4 found here, correspond to Fig. 4, 6, 7 and 8 in the main article, respectively. They display parameters of the main 2 mm aggregate data, that was discussed, but not shown in the main article.

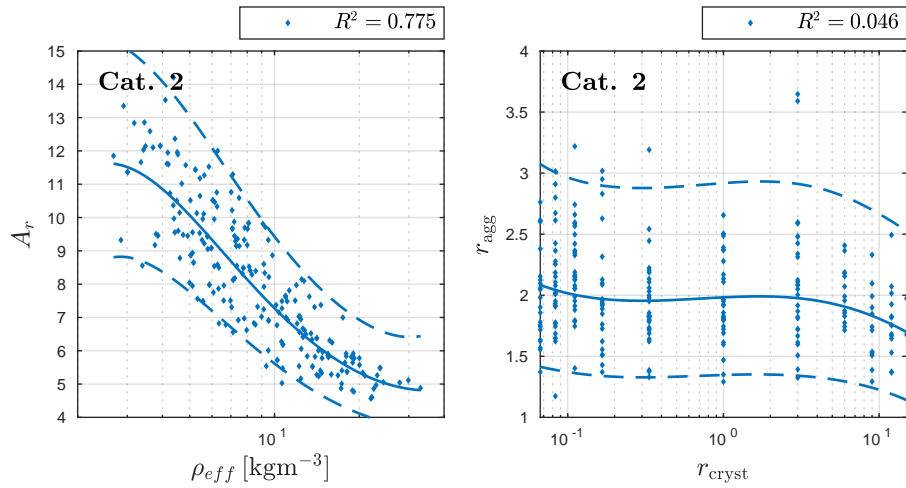


Figure 1: Aggregate parameters of category 2 shape data. (Left) Aerodynamic area ratio  $A_r$  as a function of particle effective density  $\rho_{eff}$ , using category 2 data. (Right) Aggregate aspect ratio  $r_{agg}$  as a function of crystal axis ratio  $r_{cryst}$ , using category 2 data. Lines represents cubic fits.

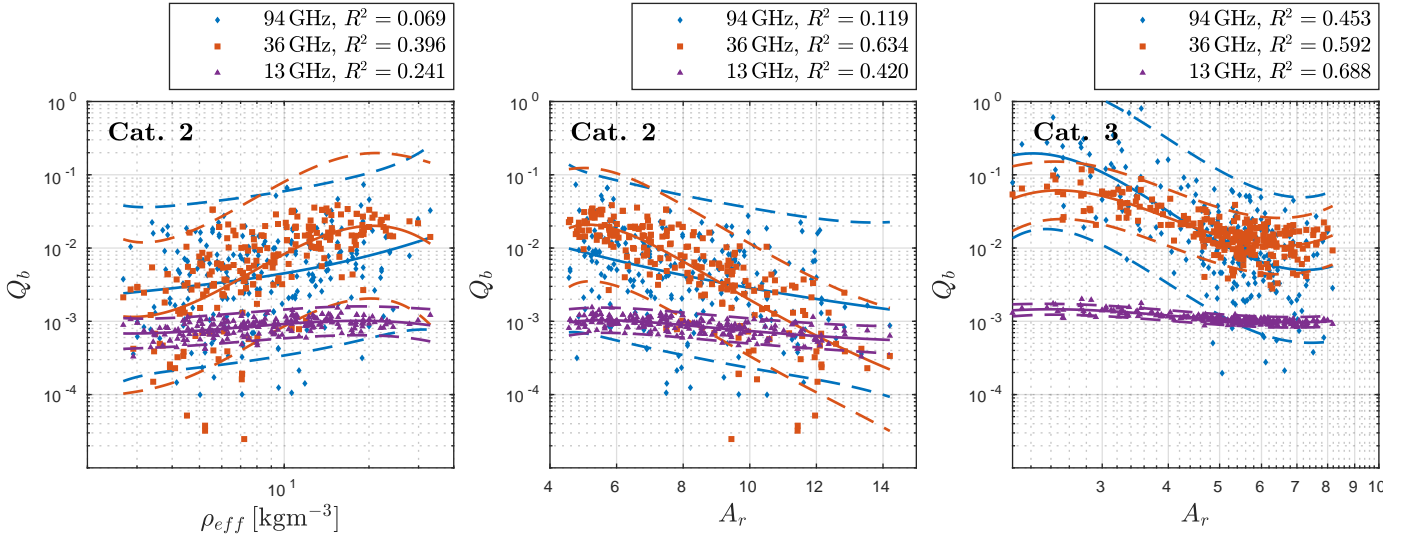


Figure 2: Back-scattering efficiencies  $Q_b$  as a function of different parameters, at 13.4, 35.6 and 94.1 GHz. The temperature is 230 K. (Left)  $Q_b$  as a function of particle effective density  $\rho_{eff}$ , using category 2 data. (Middle)  $Q_b$  as a function of function of aerodynamic area ratio  $A_r$ , using category 2 data. (Right)  $Q_b$  as a function of aerodynamic area ratio  $A_r$ , using category 3 data.

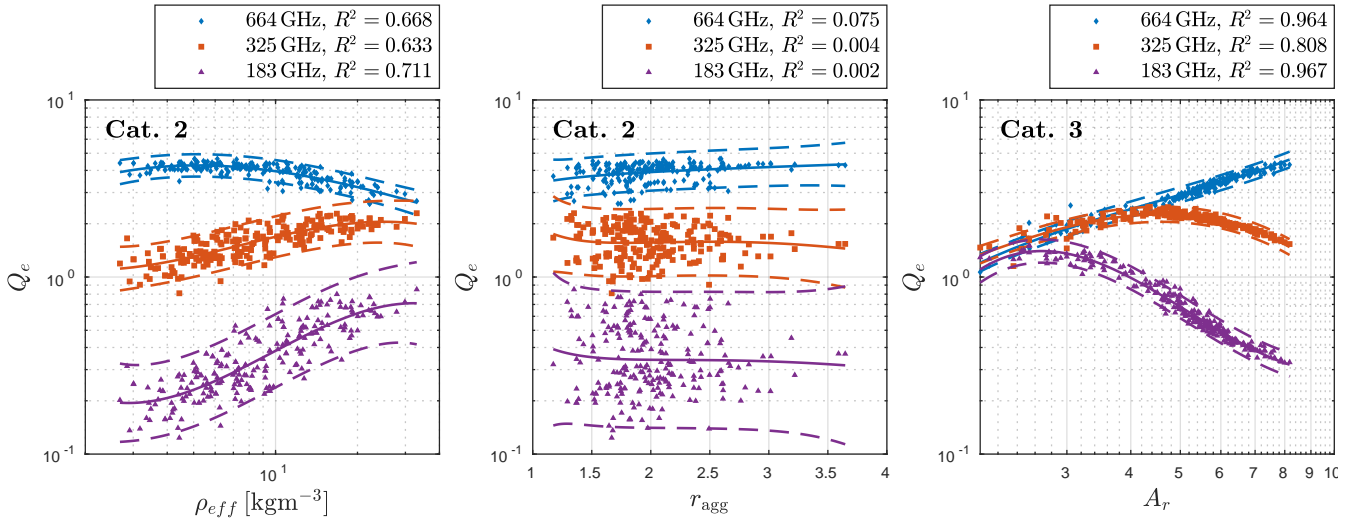


Figure 3: Extinction efficiencies  $Q_e$  as a function of different parameters, at 183.31, 325.15 and 664.00 GHz. The temperature is 230 K. (Left)  $Q_e$  as a function of particle effective density  $\rho_{eff}$ , using category 2 data. (Middle)  $Q_e$  as a function of aggregate aspect ratio  $r_{agg}$ , using category 2 data. (Right)  $Q_e$  as a function of aerodynamic area ratio  $A_r$ , using category 3 data. In contrast to corresponding figures in the main text, particles at 0.5 mm are included instead of 2 mm.

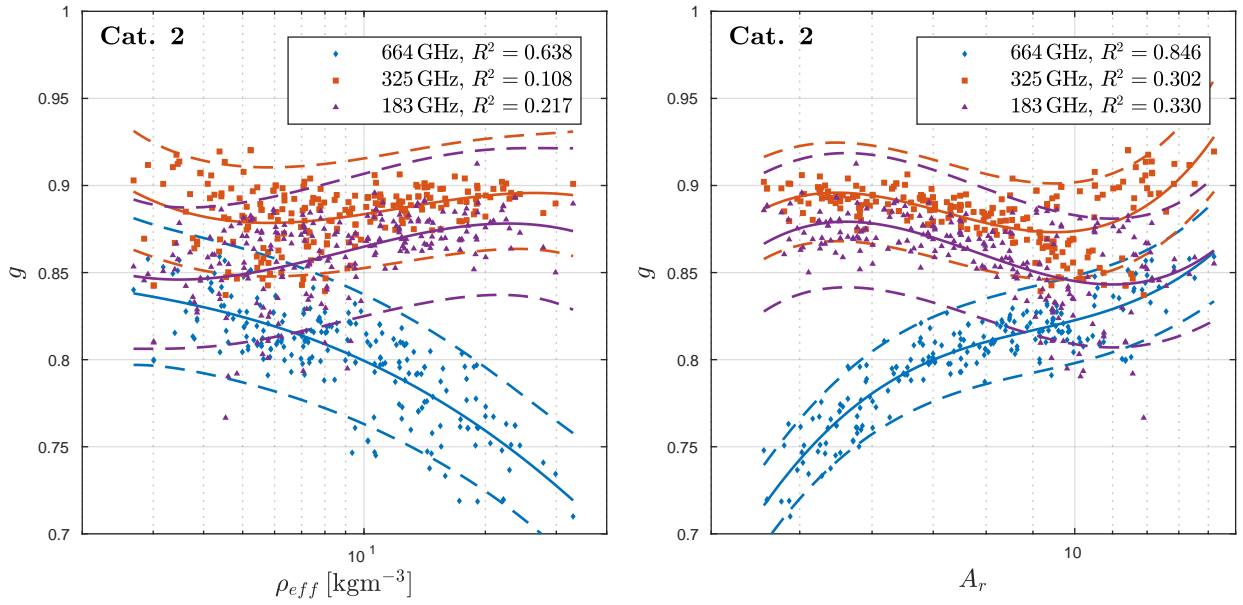


Figure 4: Asymmetry parameter  $g$  as a function of different parameters, at 183.31, 325.15 and 664.00 GHz, and a temperature of 230 K. (Left)  $g$  as a function of particle effective density  $\rho_{eff}$ , using category 2 data. (Right)  $g$  as a function of aerodynamic area ratio  $A_r$ , using category 2 data.

## 2 500 mm data

Fig. 5, 6, 7 and 8 found here, corresponds Fig. 4, 6, 7 and 8 of the main article, respectively. The difference is that all data have  $D_{\text{veq}}$  equal to 0.5 mm (as opposed to 2 mm as in the article).

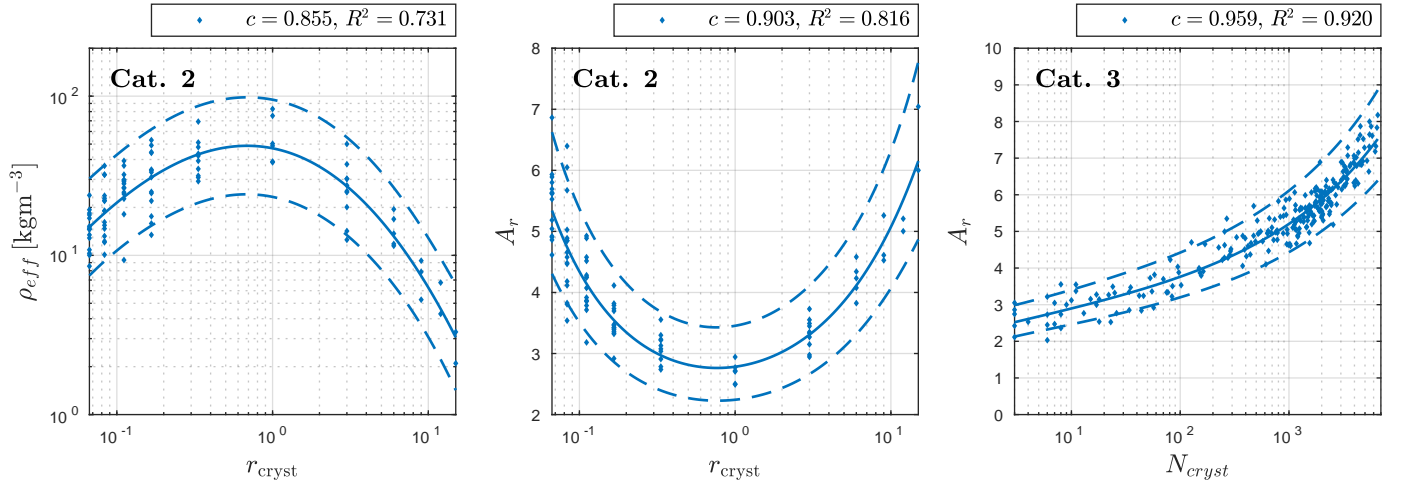


Figure 5: Aggregate parameters of category 2 and 3 shape data. (Left) Particle effective density  $\rho_{\text{eff}}$  as a function of crystal axis ratio  $r_{\text{cryst}}$ , using category 2 data. (Middle) Aerodynamic area ratio  $A_r$  as a function of  $r_{\text{cryst}}$ , using category 2 data. (Right) Aerodynamic area ratio  $A_r$  as a function of the number of constituent crystals  $N_{\text{cryst}}$ , using category 3 data. In contrast to corresponding figures in the main text, particles at 0.5 mm are included instead of 2 mm.

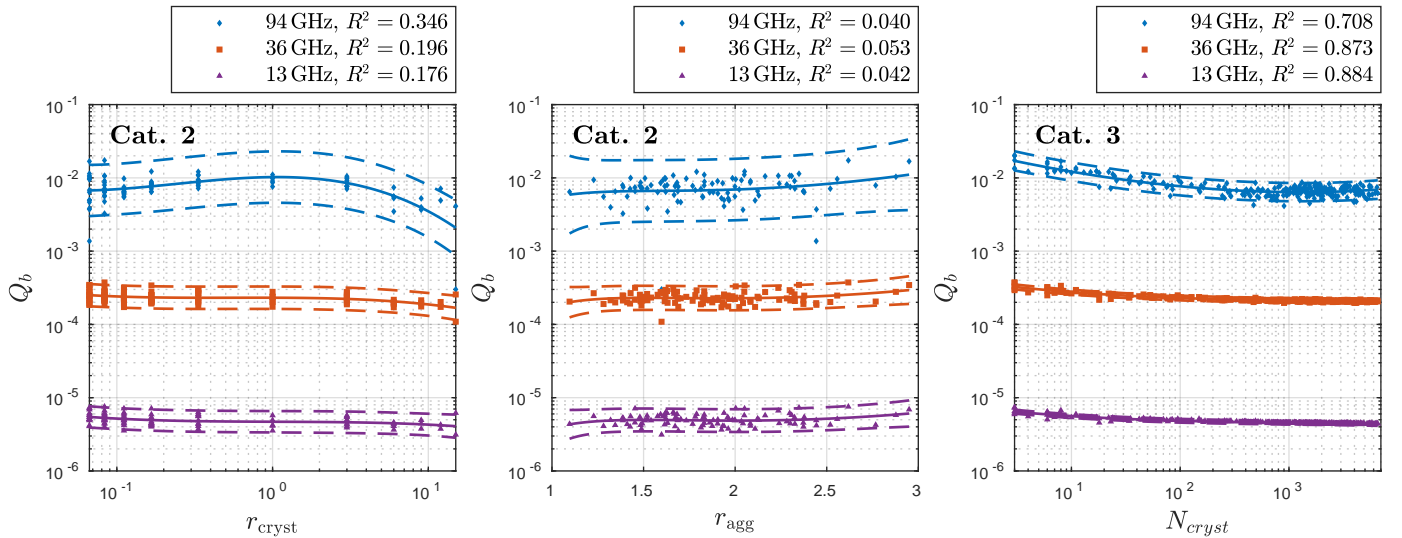


Figure 6: Back-scattering efficiencies  $Q_b$  as a function of different parameters, at 13.4, 35.6 and 94.1 GHz. The temperature is 230 K. (Left)  $Q_b$  as a function of crystal axis ratio  $r_{\text{cryst}}$ , using category 2 data. (Middle)  $Q_b$  as a function of aggregate aspect ratio  $r_{\text{agg}}$ , using category 2 data. (Right)  $Q_b$  as a function the crystal number  $N_{\text{cryst}}$ , using category 3 data. In contrast to corresponding figures in the main text, particles at 0.5 mm are included instead of 2 mm.

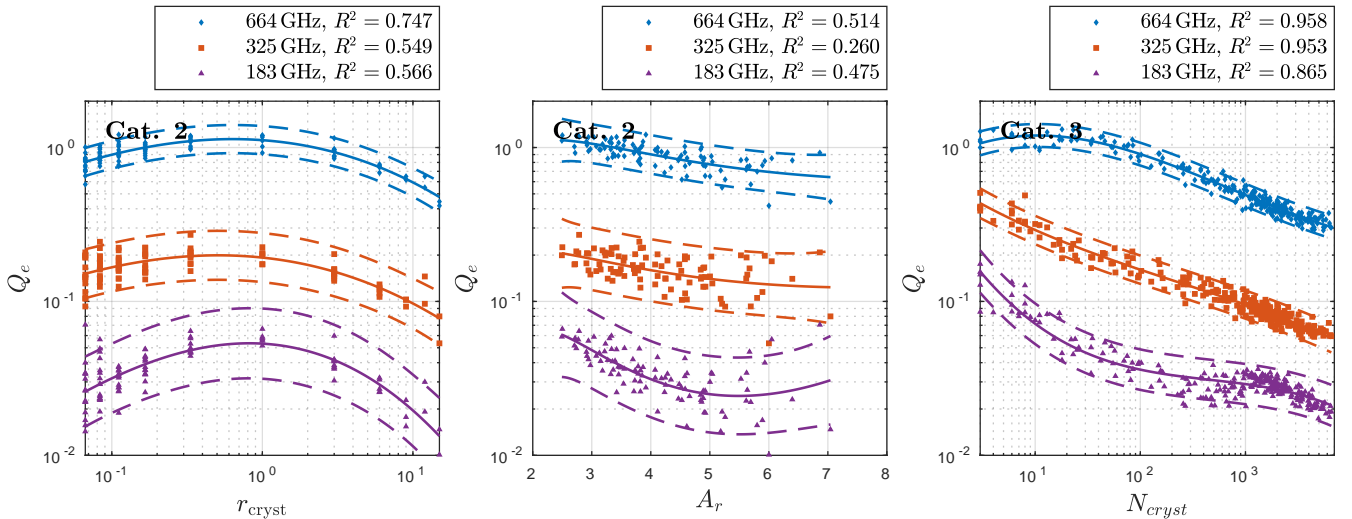


Figure 7: Extinction efficiencies  $Q_e$  as a function of different parameters, at 183.31, 325.15 and 664.00 GHz. The temperature is 230 K. (Left)  $Q_e$  as a function of crystal axis ratio  $r_{cryst}$ , using category 2 data. (Middle)  $Q_e$  as a function of aerodynamic area ratio  $A_r$ , using category 2 data. (Right)  $Q_e$  as a function of the constituent crystal number  $N_{cryst}$ , using category 3 data. In contrast to corresponding figures in the main text, particles at 0.5 mm are included instead of 2 mm.

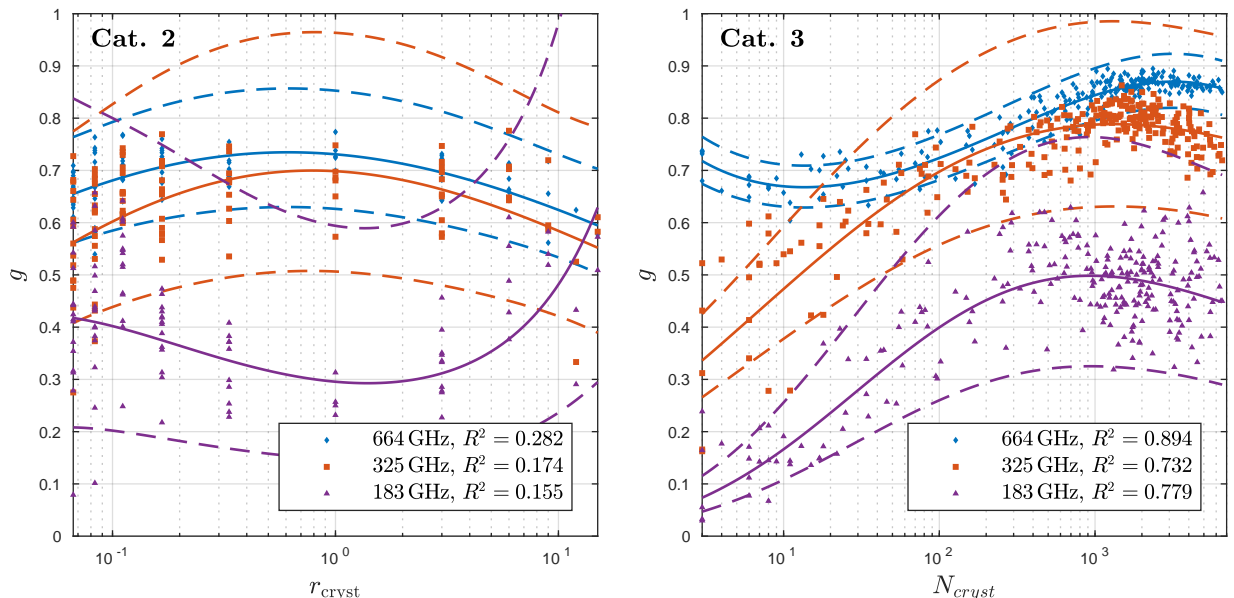


Figure 8: Asymmetry parameter  $g$  as a function of different parameters, at 183.31, 325.15 and 664.00 GHz, and a temperature of 230 K. (Left)  $g$  as a function of crystal axis ratio  $r_{cryst}$ , using category 2 data. (Right)  $g$  as a function of the crystal number  $N_{cryst}$ , using category 3 data. In contrast to corresponding figures in the main text, particles at 0.5 mm are included instead of 2 mm.

### 3 1 mm data

Fig. 9, 10, 11 and 12 found here, corresponds Fig. 4, 6, 7 and 8 of the main article, respectively. The difference is that all data have  $D_{\text{veq}}$  equal to 1 mm (as opposed to 2 mm as in the article).

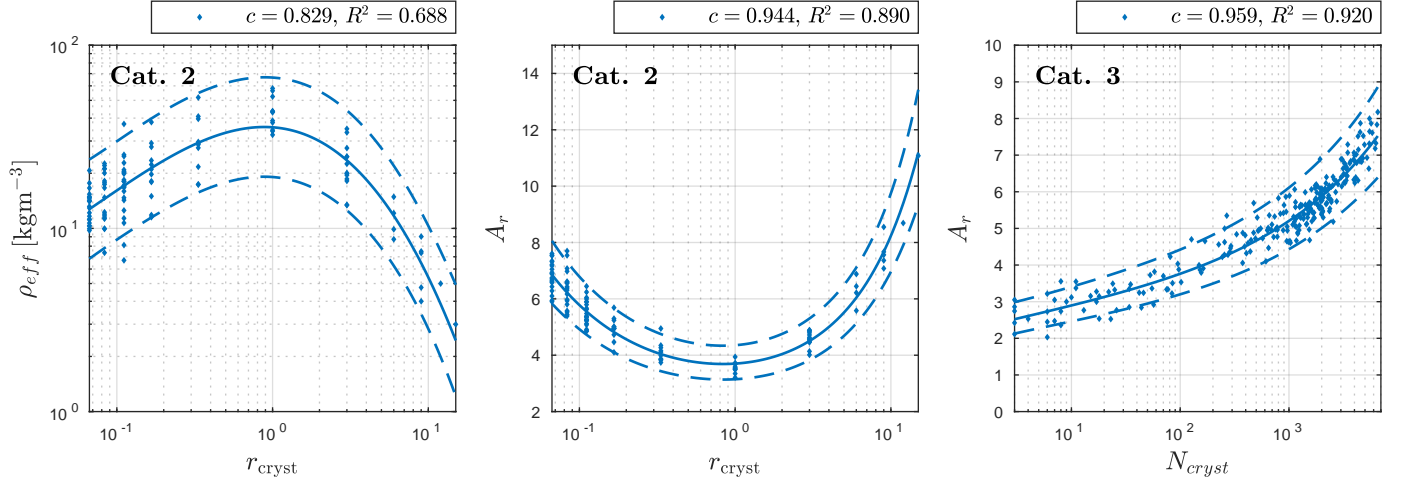


Figure 9: Aggregate parameters of category 2 and 3 shape data. (Left) Particle effective density  $\rho_{\text{eff}}$  as a function of crystal axis ratio  $r_{\text{cryst}}$ , using category 2 data. (Middle) Aerodynamic area ratio  $A_r$  as a function of  $r_{\text{cryst}}$ , using category 2 data. (Right) Aerodynamic area ratio  $A_r$  as a function of the number of constituent crystals  $N_{\text{cryst}}$ , using category 3 data. In contrast to corresponding figures in the main text, particles at 1 mm are included instead of 2 mm.

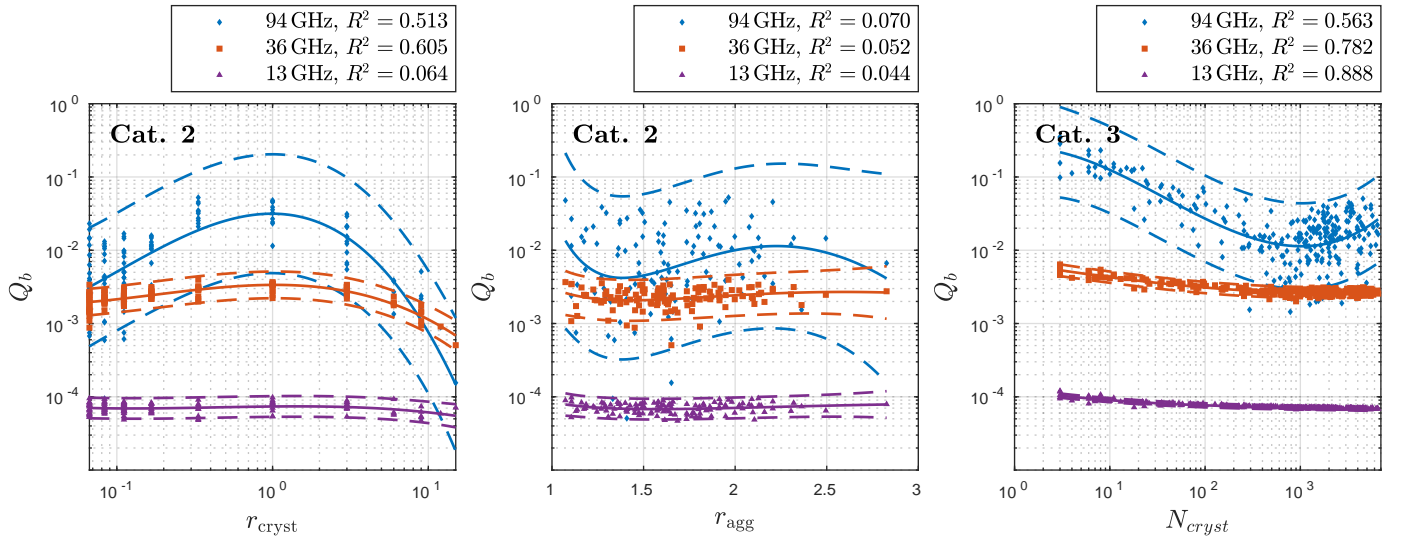


Figure 10: Back-scattering efficiencies  $Q_b$  as a function of different parameters, at 13.4, 35.6 and 94.1 GHz. The temperature is 230 K. (Left)  $Q_b$  as a function of crystal axis ratio  $r_{\text{cryst}}$ , using category 2 data. (Middle)  $Q_b$  as a function of aggregate aspect ratio  $r_{\text{agg}}$ , using category 2 data. (Right)  $Q_b$  as a function the crystal number  $N_{\text{cryst}}$ , using category 3 data. In contrast to corresponding figures in the main text, particles at 1 mm are included instead of 2 mm.

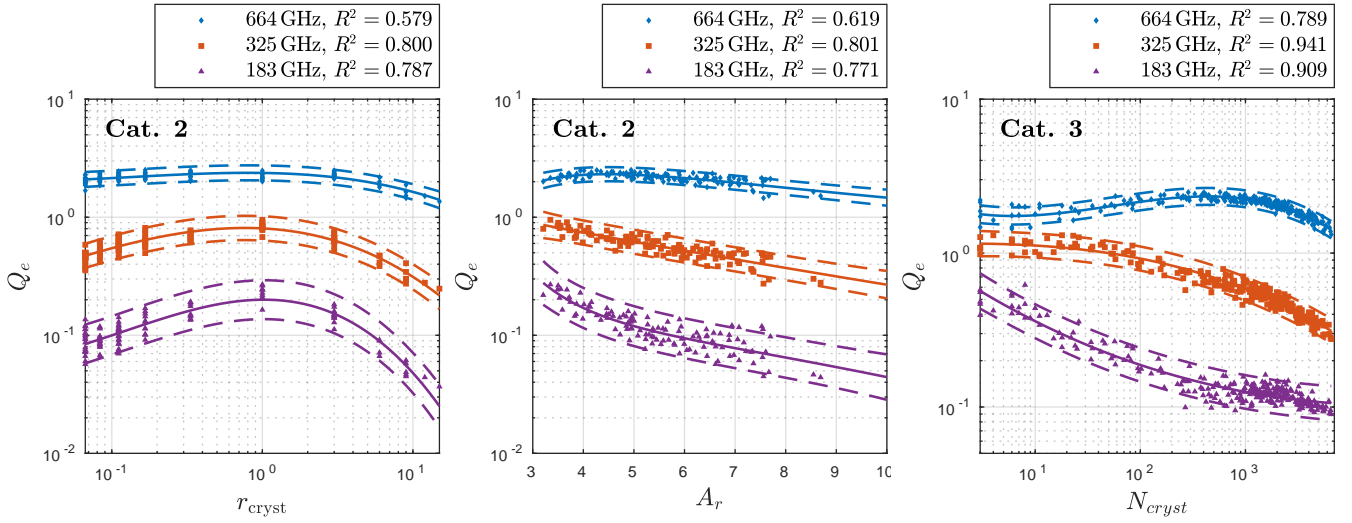


Figure 11: Extinction efficiencies  $Q_e$  as a function of different parameters, at 183.31, 325.15 and 664.00 GHz. The temperature is 230 K. (Left)  $Q_e$  as a function of crystal axis ratio  $r_{cryst}$ , using category 2 data. (Middle)  $Q_e$  as a function of aerodynamic area ratio  $A_r$ , using category 2 data. (Right)  $Q_e$  as a function of the constituent crystal number  $N_{cryst}$ , using category 3 data. In contrast to corresponding figures in the main text, particles at 1 mm are included instead of 2 mm.

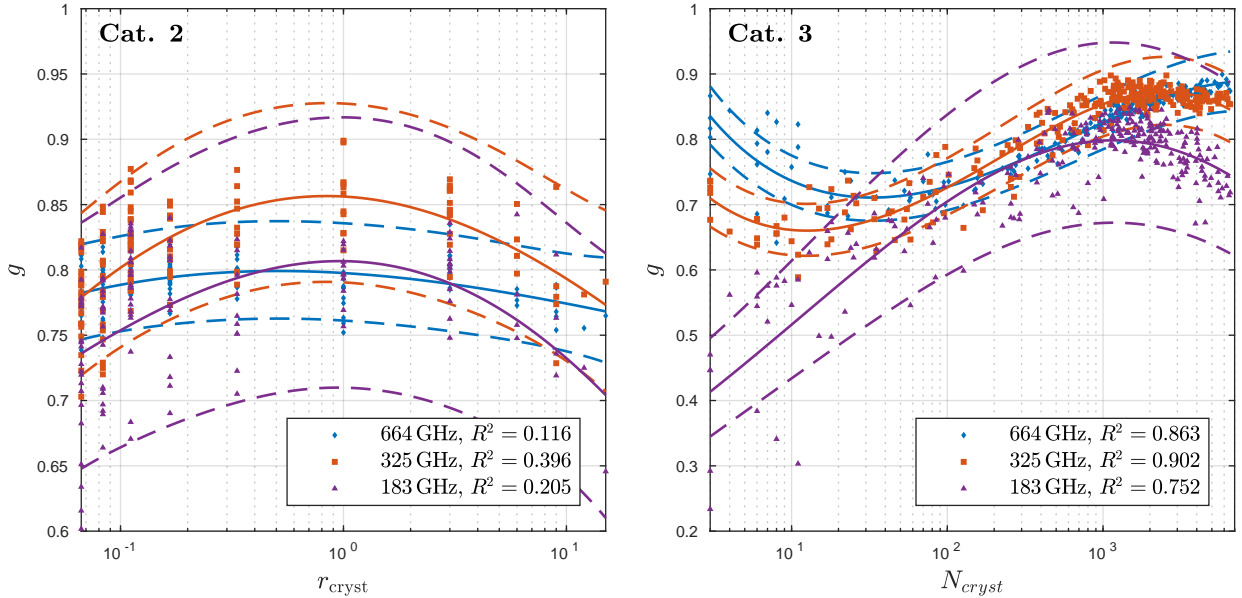


Figure 12: Asymmetry parameter  $g$  as a function of different parameters, at 183.31, 325.15 and 664.00 GHz, and a temperature of 230 K. (Left)  $g$  as a function of crystal axis ratio  $r_{cryst}$ , using category 2 data. (Right)  $g$  as a function of the crystal number  $N_{cryst}$ , using category 3 data. In contrast to corresponding figures in the main text, particles at 1 mm are included instead of 2 mm.

## 4 Alternative triple frequency signature plot

Fig. 13 corresponds to the top panel of Fig. 10 in the main article. The difference is that the particle size distribution is defined in  $D_{\max}$ , instead of  $D_{\text{veq}}$ .

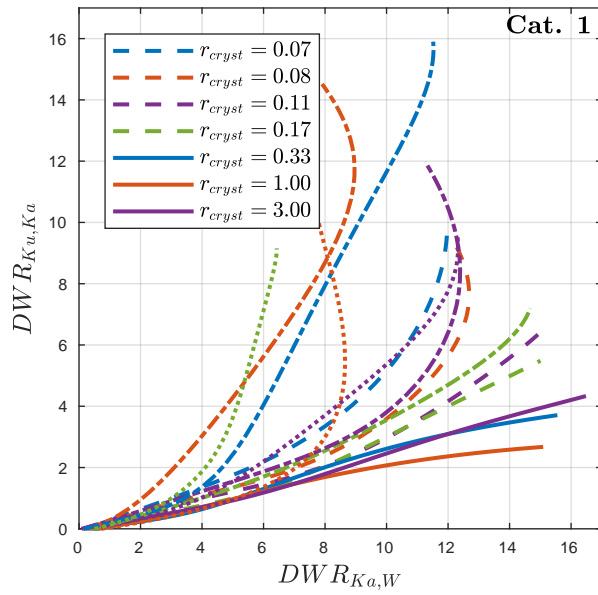


Figure 13: Triple frequency signatures using radar frequencies of 13.4 (K<sub>u</sub>-band), 35.6 (K<sub>a</sub>-band) and 94.1 GHz (W-band). Temperature is 230 K and an exponential PSD (using  $D_{\max}$  as a size parameter instead) was assumed. Lines are divided into different  $r_{\text{cryst}}$ -values. (Top) Triple frequency signatures.